Honours Thesis - Proposal and Preparation - PHYS 4676

CRN: 18138
Duration: Sep 04, 2014 - Dec 03, 2014
Credits: 3

Instructor for the course:

Dr. Can-Ming Hu
Professor
Department of Physics and Astronomy
University of Manitoba,
Winnipeg, Manitoba,
Canada R3T 2N2

Telefon: (001) 204 - 474 6189
Email: hu@physics.umanitoba.ca
Website: http://www.physics.umanitoba.ca/~hu
Office: Allen 332, availability for individual student consultation:*anytime when I am in the office*

Project supervisors for the course:

Dr. Can-Ming Hu, Dr. Stephen Pistorius, Dr. Kumar Sharma, Dr. Johan van Lierop.

Course and project materials:

Each student should discuss with their project supervisor about the materials.

Evaluation procedure and a tentative schedule of the exam:

Each student should prepare **an oral presentation** and **a written proposal** for their Honours Thesis research. The final course grade will be determined from the student's performance in both, with an **equal weight**.

The oral presentation will be given in a block seminar on Wednesday Dec 10th, 2:00 pm – 4:30 pm (room: 326 Allen). All students of this course are expected to participate in the block seminar. Before the block seminar, each student should make appointment individually with their project supervisor, presenting their slides, and get their slides and preparation evaluated by their project supervisor (**40%**). At the block seminar, each presentation consists of 20 min presentation plus 10 min Q/A, which will be evaluated by the course instructor (**40%**) and all other students (**20%**, averaged by all of them). The evaluation sheet is attached. After the block seminar, the students may revise their slides based on the discussions. The revised slides in PDF format must be submitted to the course instructor by the end of Friday, Dec. 12th. Late submission will receive 10% penalty of the mark.

The written proposal will be evaluated by the course instructor (**50%**) and the project supervisor (**50%**). The written proposal in PDF format must be submitted to both the course

instructor and the project supervisor by the end of Friday Dec. 12th. Late submission will receive 10% penalty. An example with the appropriate formatting and referencing style is attached.

Academic Integrity

Students are expected to conduct themselves in accordance with the highest ethical standards and evince academic integrity in all their pursuits and activities at the university. As such in accordance with the General Academic Regulations and Requirements of the University of Manitoba, Section 7.1, students are reminded that "plagiarism or any other form of cheating in examinations or term tests (e.g. crib notes) is subject to serious academic penalty (e.g. suspension or expulsion from the faculty or university). A student found guilty of contributing to cheating in examinations or term assignments is also subject to serious penalty."

PHYS4676 Oral Presentation Evaluation Sheet (Wednesday, Dec 10th, 2014) Name: _____

Speaker	2:00-2:30 Blanchette, Keagan A.	2:30-3:00 Guo, Kaiming	3:00-3:30 Kaur, Sandeep	3:30-4:00 Reimer, Alex J.	4:00-4:30 Rutley, Christopher B.	
Project Supervisor	Hu	Pistorious	Hu	Sharma	Van Lierop	
Thesis Introduction Max: 20						
Objective and Method Max: 20						
Thesis Plan & Timeline Max 20						
Presentation Qualities Max 20						
Answer to questions Max 20						
Total (Max: 100)						
Course Instructor (40%)						
Project Supervisor (40%)						
Avg of all others (20%)						
Total Mark						

The Line Shape of Electrically Detected Ferromagnetic Resonance

Michael Harder

December 17, 2010

(PHYS 4676)

A proposal submitted to the Department of Physics & Astronomy in partial fulfillment of the requirements for the Honours Physics Thesis

1 Introduction

Ferromagnetic resonance (FMR) was first discovered in the early 20^{th} century when certain ferromagnetic films were found to strongly absorb microwave frequency electromagnetic radiation [1]. This spectroscopic technique allows researchers to probe the spin properties (both locally and macroscopically) of a material and has become a standard tool in the research of spin dynamics making it invaluable to the field of spintronics. Recently the electrical detection of FMR has gained popularity amongst the spintronics community and has proven to be a powerful experimental tool [2]. However to properly characterize the electrically detected ferromagnetic resonance both the FMR voltage and FMR line shape must be determined. The later requires knowledge of the relative electromagnetic phase Φ, which has proven difficult to measure since the introduction of Maxwell's theory. This lack of experimental experience with Φ has led to misconceptions regarding its importance in FMR experiments, which have recently begun to surface in the literature [7]. Not only is the relative electromagnetic phase vital to properly performing FMR experiments, but Φ also provides a coherent link between electrodynamics and magnetodynamics and as such has a broad physical relevance, motivating a clear understanding. However, in order to measure this relative phase one must probe both the electric and magnetic processes at the same time in the same device, and until recently this was not possible. However with the advent of spintronic Michelson interferometry this ability has been realized. By combining this novel experimental technique with a clear theoretical understanding we propose to systematically demonstrate the Φ dependence of the FMR line shape and to provide a foundation with which to properly understand the influence of the relative electromagnetic phase.

2 Motivation - Spin Hall Effect

Driving the clear understanding of the FMR line shape is the important role FMR spectroscopy has come to play in the rapidly developing field of spintronics, in particular in the study of the spin Hall effect (SHE). The spin Hall effect, theoretically described in 1971 by D'yakonov and Perel [23, 24], but only observed in 2004 [25, 26] has garnered great interest amongst the condensed matter community due to its ability to convert charge currents into spin currents and vice versa, suggesting great potential in the field of spintronics. The SHE in a conductor is due to the spin dependent scattering of charge carriers originating from the spin-orbit interaction, which causes spin-up and spin-down electrons to flow in opposite directions resulting in a net spin accumulation [7]. If the conductor has equal up and down spin densities, the equal and opposite Hall charge currents will cancel, leaving only a pure spin current [8]. Alternatively spin pumping can drive pure spin currents. As described by Tserkovnyak *et. al.* [9, 10] magnetization precession at a ferromagnetic-normal metal (F|N) interface can act as a spin pump which transfers a spin current from the ferromagnet into the normal metal. Such a spin current can be converted back into a charge current through the inverse spin Hall effect via the spin-orbit interaction and the effectiveness of this spin-charge conversion can be characterized by the spin Hall angle γ, which is the ratio of spin Hall and charge conductivities.

An accurate determination of γ has broad applications to spintronics, since the conversion between spin and charge currents determined by γ is the key to developing spin driven electronic, or spintronic devices. By converting the spin pumping current into a charge current through the SHE a spin battery could be enabled and could be used to power electronic devices [11, 12, 13]. Such spin powered devices are characterized by their low power consumption and small size and as such are the future of electronics. However experimentally determining γ has proven controversial. For example, work by Seki *et. al.* found a large spin Hall angle in Au of $\gamma = 0.113$ suggesting the giant SHE [14] , however Mihajlovic *et. al.* found an upper limit for γ

in Au under similar conditions to be 0.023 [15]. Similarly in Pt the spin Hall angle was found to be 0.08 and 0.0037 by Ando *et. al.* [16] and Kimura *et. al.* [17] respectively. Clearly this indicates a lack of understanding in characterizing the SHE, which is largely due to limitations in measurement methodology. In particular, in such spin pumping experiments there exist other voltages, such as a voltage produced by the anisotropic magnetoresistance (AMR), in addition to the spin Hall voltage and the proposed measurement schemes must account for this [18, 19]. The discrepancies in the measured spin Hall angles are likely due to improperly distinguishing these different voltage producing effects.

In configurations where the AMR and SHE dominate, the voltages are typically distinguished based on the symmetry or antisymmetry of the FMR lineshape [7]. However since the AMR voltage depends on the relative electromagnetic phase, while the spin Hall voltage does not, proper characterization of the line shape symmetry depends on the value of Φ, which from basic electromagnetism is known to be material and frequency dependent and will thus be different for each apparatus. This suggests that the spin Hall angle cannot be properly determined from the FMR line shape without characterizing the relative electromagnetic phase first. In some recent experiments both effects have been included in the data analysis [7], however the AMR effect has been added only as a convenient way of explaining the observed antisymmetric line shape component of the FMR (since the SHE is predicted to produce a purely symmetric line shape) and the general AMR effect which produces both a symmetric and antisymmetric line shape has been ignored. Thus a clear picture of the Φ influence on spintronic measurements is still lacking and is necessary to confidently determine γ. Through the proposed work such a picture will be painted in three steps: by showing through a model calculation that there is a relative phase shift in a thin film multilayer system, by theoretically describing the FMR line shape and showing its phase dependence and experimentally by measuring Φ for various samples through the use of electrically detected FMR and spintronic Michelson interferometry.

3 Theory

3.1 Ferromagnetic Resonance

The source of ferromagnetism is the spontaneous magnetic moment possessed by certain materials below the Curie temperature, T_C. This spin polarization arises from the exchange interaction which makes it energetically favorable for the spins of neighboring atoms to align [3, 4] resulting in a locally non-zero magnetic moment per volume, or magnetization. The application of an external dc magnetic field can be used to enhance this effect and globally align the magnetization of a sample with the field direction and by applying an additional rf field the magnetization can be driven to precess around this equilibrium position. This precession is phenomenologically described by the semi classical Landau Lifshitz Gilbert (LLG) equation,

$$\frac{d\mathbf{M}}{dt} = -\gamma(\mathbf{M} \times \mathbf{H}_{eff}) - \frac{\alpha_G \gamma}{|\mathbf{M}|}[\mathbf{M} \times (\mathbf{M} \times \mathbf{H}_{eff})] \tag{1}$$

where the last term in Eq. 1 is the phenomenological Gilbert damping term with α_G being the Gilbert damping parameter and γ is the electron gyromagnetic ratio. Here $\mathbf{M}$ is the net sample magnetization, defined as the magnetic moment per unit volume, and $\mathbf{H}_{eff}$ includes all the magnetic fields seen by the electron such as fields from the exchange interaction, dipole-dipole interaction, anisotropy interaction and the externally applied field, which itself will contain a dc and rf term [5]. The Landau Lifshitz Gilbert equation attributes the cause of the magnetization motion to a torque applied by the magnetic field in analogy with the torque exerted by gravity on a precessing top [5, 6] as shown in Fig. 1.

To solve the LLG equation we define $\mathbf{M} = \mathbf{M}_0 + \mathbf{m}e^{-i\omega t}$ and $\mathbf{H}_{eff} = \mathbf{H}_0^{in} + \mathbf{h}^{in}e^{-i\omega t}$ where $\mathbf{M}_0$ is the dc magnetization (resulting mainly from the dc applied magnetic field), $\mathbf{m}e^{-i\omega t}$ is the rf magnetization (driven mainly be the applied microwave field), $\mathbf{H}_0^{in}$ is the internal dc magnetic field and $\mathbf{h}^{in}e^{-i\omega t}$ is the internal rf field. These internal fields are related to the externally applied field $\mathbf{H} = \mathbf{H}_0 + \mathbf{h}e^{-i\omega t}$ through the boundary conditions of Maxwell's equations. Since the damping is small terms

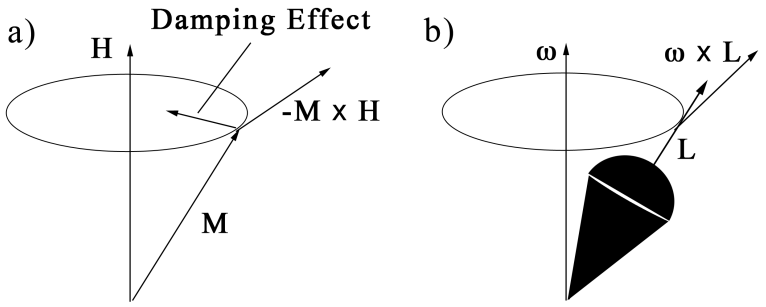

Figure 1: **a)** Precession of the magnetization **M** due to the magnetic field **H**. **b)** Precession of a spinning top due to the torque from gravity.

higher than first order in α_G can be ignored and using the linear approximation terms higher than the first power in $\mathbf{h}^{in}$ and $\mathbf{m}$ are ignored. By using these approximations along with the boundary conditions of Maxwell's equations the solution of the LLG equation yields the Polder susceptibility tensor, $\widehat{\chi}$ which relates $\mathbf{m}$ and $\mathbf{h}$ [22]

$$\mathbf{m} = \widehat{\chi}\mathbf{h} \tag{2}$$

$$\widehat{\chi} = \begin{pmatrix} \chi_{xx} & i\chi_{xy} & 0 \\ -i\chi_{xy} & \chi_{yy} & 0 \\ 0 & 0 & 0 \end{pmatrix} \tag{3}$$

The elements of $\widehat{\chi}$ are given by

$$\chi_{xx} = \frac{\omega_r\omega_M + \omega_M^2}{\omega_r(\omega_r + \omega_M) - \omega^2} \quad \chi_{xy} = \frac{\omega\omega_M}{\omega_r(\omega_r + \omega_M) - \omega^2} \quad \chi_{yy} = \frac{\omega_r\omega_M}{\omega_r(\omega_r + \omega_M) - \omega^2} \tag{4}$$

with $\omega_0 = \gamma \mathrm{H}_0$, $\omega_r = \omega_0 - i\alpha_G\omega$ and $\omega_M = \gamma \mathrm{M}_0$. This solution becomes resonant in the microwave frequency range, resulting in the effect known as ferromagnetic resonance.

3.2 Spin Rectification

Originally ferromagnetic resonance experiments were performed on bulk magnetic samples using resonance cavities where a sample would be placed in the cavity and the microwave intensity would be measured as a function of the applied magnetic field [1]. At resonance a strong absorption occurs in the sample causing a sharp decrease in the measured intensity, allowing a determination of the resonance field. This technique works remarkably well for bulk materials, and even for ferromagnetic thin films, but recently the improvement of fabrication techniques has enabled the production of thin film microstructures with dimensions small enough (on the order of 10 - 100 μm) that their effect on the intensity in the comparatively large cavity is negligible, requiring a new method of FMR detection. Fortunately the improvements in thin film fabrication have been complemented by the development of planar waveguide devices which allow precise delivery of the microwave field enabling a solution to the FMR problem by electrical detection. Such an electrical detection technique directly probes the sample properties by detecting a voltage generated via the spin rectification effect, which produces a dc voltage through the non linear coupling of rf electric and magnetic fields. It is this so called photovoltage which replaces the intensity measurement and whose line shape is of interest. This voltage production follows the generalized Ohm's law

$$\mathbf{J} = \sigma \mathbf{E}_0 - \frac{\sigma \Delta\rho}{\mathbf{M}^2}(\mathbf{J} \cdot \mathbf{M})\mathbf{M} + \sigma R_H \mathbf{J} \times \mathbf{M} \tag{5}$$

Here the first term describes the normal Ohm's law where the current $\mathbf{J}$ is linearly related to the electric field $\mathbf{E}_0$ through the conductivity σ. The last two terms represent non linear corrections to Ohm's law, where the second term describes anisotropic magnetoresistance (AMR), and the third describes the anomalous Hall effect. $\Delta\rho$ is the resistivity change corresponding to the AMR effect, and R_H is the anomalous Hall coefficient.

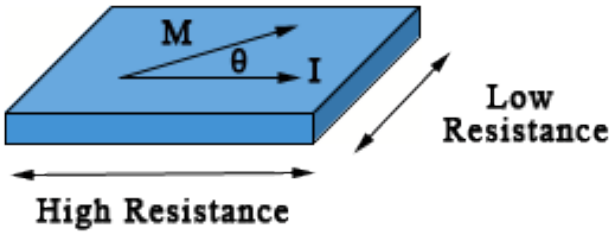

Figure 2: Anisotropic magnetoresistance effect, where the largest resistance is observed when the current and magnetization are parallel, and the smallest resistance occurs when they are perpendicular

Rewriting this equation as the sum of two fields we have

$$\mathbf{J} = \sigma(\mathbf{E}_0 + \mathbf{E}_1)$$

$$\mathbf{E}_1 = -\frac{\Delta\rho}{\mathbf{M}^2}(\mathbf{J}\cdot\mathbf{M})\mathbf{M} + R_H\mathbf{J}\times\mathbf{M} \tag{6}$$

If $\mathbf{E}_0$ is an rf field it will time average to zero, but the higher order $\mathbf{E}_1$ will in general have a non zero time average resulting in the so called rectified voltage. A static magnetic field, $\mathbf{H}_0$ is used to create a static magnetization, $\mathbf{M}_0$ and an applied microwave field $\mathbf{h}^t = (h_x^t,\, h_y^t,\, h_z^t) = (h_x e^{-i(\omega t+\Phi_x)},\, h_y e^{-i(\omega t+\Phi_y)},\, h_z e^{-i(\omega t+\Phi_z)})$ will be used to induce oscillations about this equilibrium. Here Φ_j denotes the phase shift between the electric and magnetic fields in the jth direction. To first order the applied magnetic field will result in a time dependent magnetization which is perpendicular to the static field direction, $\mathbf{m}^t = Re(\widetilde{\mathbf{m}}^t)$, where $\widetilde{\mathbf{m}}^t$ is the magnetization which comes from solving the Landau Lifshitz Gilbert equation. This results in a total magnetization $\mathbf{M} = \mathbf{M}_0 + \mathbf{m}^t$. Note that $\mathbf{m}$ is time dependent through its relation (through the LLG equation) to the time dependent microwave magnetic field, and as a result $\mathbf{m}^t$ is also time dependent although we do not explicitly include this dependence.

Using the magnetization and feld expressions in Eq. 6, we find the microwave field as the time average of $\mathbf{E}_1$

$$\mathbf{E}_{MW} = \langle \mathbf{E}_1 \rangle = \frac{-\Delta\rho}{M_0^2} \left\langle \left(\mathbf{J} \cdot \mathbf{m}^t\right) \mathbf{M}_0 + \left(\mathbf{J} \cdot \mathbf{M}_0\right) \mathbf{m}^t \right\rangle + R_H \left\langle \mathbf{J} \times \mathbf{m}^t \right\rangle \tag{7}$$

Eq. 7 gives the general microwave field expression from which the photovoltage and its line shape can be determined.

3.2.1 In Plane H Field

In the case of a thin film microstructure where the sample thickness is much less than the length and width, effectively resulting in a 2D plane, it is useful to define two field configurations, namely in plane and out of plane, which we will use to excite FMR in our experiments. The line shape for each of these configurations

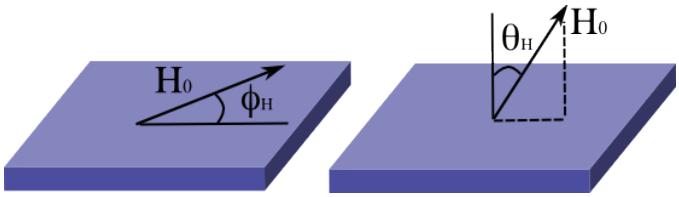

Figure 3: The two field configurations for a thin ferromagnetic film. Here $\mathbf{H}_0$ is the externally applied dc magnetic field, ϕ_H is the in plane field angle and θ_H is the perpendicular field angle.

can be determined from Eq. 7. In the case of an in plane field we consider the two coordinate systems in Fig. 4. Here the dc field and resulting static magnetization are denoted by $\mathbf{H}_0$ and $\mathbf{M}_0$ respectively. The z axis is along the field direction while the z' axis is along the current direction. The two coordinate systems are related through the transformation

$$\begin{pmatrix} \widehat{\mathbf{x}} \\ \widehat{\mathbf{y}} \\ \widehat{\mathbf{z}} \end{pmatrix} = \begin{pmatrix} cos(\phi_H) & 0 & -sin(\phi_H) \\ 0 & 1 & 0 \\ sin(\phi_H) & 0 & cos(\phi_H) \end{pmatrix} \begin{pmatrix} \widehat{\mathbf{x}'} \\ \widehat{\mathbf{y}'} \\ \widehat{\mathbf{z}'} \end{pmatrix} \tag{8}$$

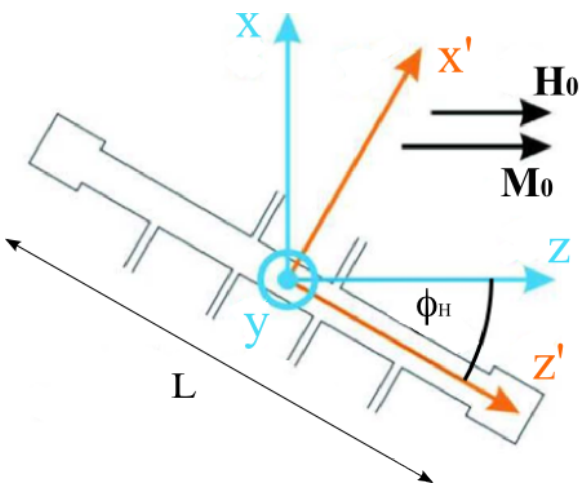

Figure 4: Coordinate systems for in plane magnetic field.

Using this field configuration we have $\mathbf{m}^t = (\mathrm{m}_x^t,\ \mathrm{m}_y^t,\ 0)$ and due to the strip geometry the current flows along the z' direction and is given by $\mathbf{J} = \mathrm{j}_z' \cos(\omega \mathrm{t})\widehat{\mathbf{z}'}$. Using these expressions in Eq. 7, and transforming $\mathbf{m}^t$ to the primed coordinate system the time averaged microwave electric field is given by

$$\begin{aligned}\mathbf{E}_{MW} = &-\frac{\Delta\rho}{M_0^2}\left\langle -M_0 j_{z'} cos(\omega t) m_x^t sin(\phi_H)\left[sin(\phi_H)\widehat{\mathbf{x}'} + cos(\phi_H)\widehat{\mathbf{z}'}\right]\right\rangle \\ &-\frac{\Delta\rho}{M_0^2}\left\langle M_0 j_{z'} cos(\omega t) cos(\phi_H)\left[m_x^t cos(\phi_H)\widehat{\mathbf{x}'} + m_y^t\widehat{\mathbf{y}'} - m_x^t sin(\phi_H)\widehat{\mathbf{z}'}\right]\right\rangle \\ &+R_H\left\langle -j_{z'} cos(\omega t) m_y^t\widehat{\mathbf{x}'} + j_{z'} cos(\omega t) m_x^t cos(\phi_H)\widehat{\mathbf{y}'}\right\rangle \end{aligned} \tag{9}$$

To find the voltage in the ferromagnetic strip we then simply integrate the field along the length of the strip.

$$V = \int_0^L \mathbf{E}_{MW}\cdot d\mathbf{z}' = L\mathbf{E}_{MW}\cdot\widehat{\mathbf{z}'}$$

$$V = \frac{\Delta R}{M_0}\left\langle I_{z'} cos(\omega t) m_x^t\right\rangle sin(2\phi_H) \tag{10}$$

Here we have used $I_{z'} = A j_{z'}$ and $\Delta R = \Delta\rho\frac{L}{A}$ where A is the cross sectional area. Now returning to the solution of the LLG equation (Eq. 3), we know that m_x^t is

related to the applied microwave field, $m_x^t = Re(|\chi_{xx}|e^{-i\Theta}h_x^t + i|\chi_{xy}|e^{-i\Theta}h_y^t)$. Where Θ is the spin resonance phase which changes from 180° (driving force out of phase with precession) to 0° (driving force in phase) around resonance, going through 90° at resonance. Combining this relationship with the microwave magnetic field expression and Eq. 10 the in plane voltage is given by

$$V = \frac{\Delta R}{M_0} I_{z'} sin(2\phi_H) \left[|\chi_{xx}|h_{x'}cos(\phi_H)cos(\Phi_{x'} + \Theta) - |\chi_{xx}|h_{z'}cos(\Phi_{z'} + \Theta)sin(\theta_H) \right.$$
$$\left. -|\chi_{xy}|h_{y'}sin(\Phi_{y'} + \Theta)\right] \quad (11)$$

In the appropriate experimental conditions, the dominant contribution to the driving microwave field is the $h_{x'}$ field and we may take $h_{y'} \rightarrow 0$ and $h_{z'} \rightarrow 0$ which leaves

$$V = \frac{\Delta R}{M_0} I_{z'} sin(2\phi_H)|\chi_{xx}|h_{x'}cos(\phi_H)cos(\Phi_{x'} + \Theta) \quad (12)$$

3.2.2 Out of Plane H Field

For an out of plane field we use the two coordinate systems shown in Fig. 5 where the two coordinate systems are related by

$$\begin{pmatrix} \widehat{\mathbf{x}} \\ \widehat{\mathbf{y}} \\ \widehat{\mathbf{z}} \end{pmatrix} = \begin{pmatrix} 1 & 0 & 0 \\ 0 & cos(\phi_H) & -sin(\phi_H) \\ 0 & sin(\phi_H) & cos(\phi_H) \end{pmatrix} \begin{pmatrix} \widehat{\mathbf{x}'} \\ \widehat{\mathbf{y}'} \\ \widehat{\mathbf{z}'} \end{pmatrix} \quad (13)$$

In this case $\mathbf{M}_0$ = (0, M_0, 0) and $\mathbf{m}^t$ = (m_x^t, 0, m_z^t) and again $\mathbf{J} = j_{z'}\cos(\omega t)\widehat{\mathbf{z}'}$. Following through with the same approach as the in plane case using Eq. 7 the voltage is given by

$$V = -\frac{\Delta R}{M_0} I_{z'} sin(2\theta_H) \left[|\chi_{xy}|h_{x'}sin(\theta_H)sin(\Phi_{x'} + \Theta) - |\chi_{yy}|h_{y'}sin(\theta_H)cos(\Phi_{y'} + \Theta)\right] \quad (14)$$

Here the dominant contribution will be due to $h_{x'}$ and taking $h_{y'} \rightarrow 0$ the voltage expression becomes

$$V = -\frac{\Delta R}{M_0} I_{z'} sin(2\theta_H)|\chi_{xy}|h_{x'}sin(\theta_H)sin(\Phi_{x'} + \Theta) \quad (15)$$

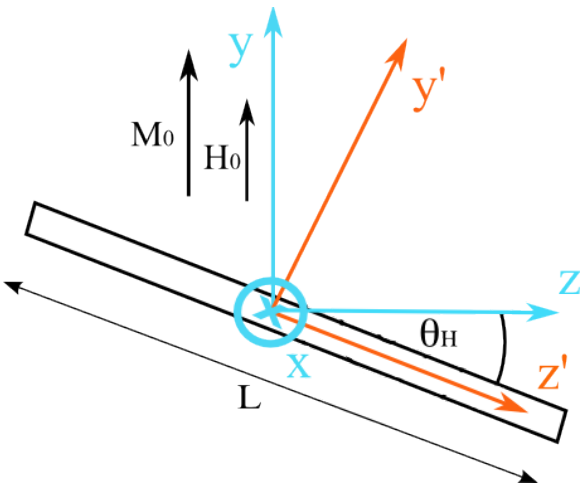

Figure 5: Coordinate systems for out of plane magnetic field.

Eq. 12 and Eq. 15 give the expressions we will use to fit the in plane and out of plane FMR line shapes respectively. We see that in the in plane configuration the photovoltage is due to m_x^t driven by $h_{x'}^t cos(\phi_H)$ whereas in the perpendicular configuration the photovoltage is due to m_z^t driven by $h_{x'}^t$. A feature common to both expressions is that at certain points of high symmetry there will be no voltage production. For both the in plane and perpendicular configurations this occurs at ϕ_H, $\theta_H = n\frac{\pi}{2}$ $n = 0, 1, 2, \ldots$. When exciting FMR we will have to avoid these points.

4 Experimental Method

4.1 Spintronic Michelson Interferometry

As mentioned previously the difficulties associated with the direct measurement of the relative electromagnetic phase have long prohibited experimentally probing Φ. However the novel technique of spintronic Michelson interferometry allows such a measurement by transforming the well known Michelson interferometry technique into a powerful phase resolved spintronic probe. This technique has the ability to

coherently measure both the electro and magneto dynamic processes at the same time, in the same ferromagnetic sample, and it is this capability which can be used to probe the relative electromagnetic phase Φ.

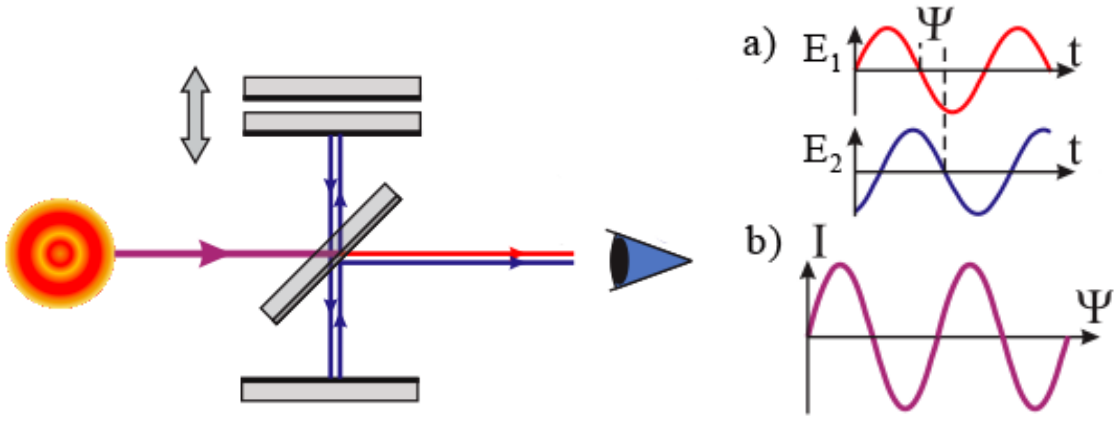

Figure 6: Classical Michelson Interferometer. **a)** The two electric fields and their phase shift Ψ which results in the interference pattern in **b)**.

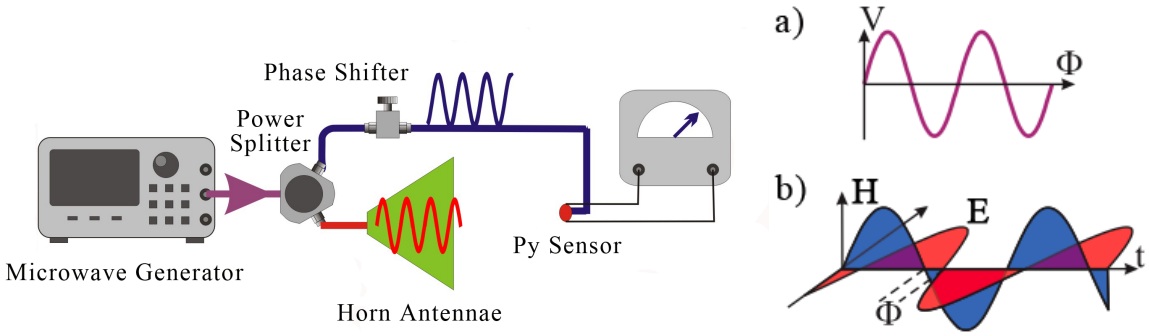

Figure 7: Spintronic Michelson Interferometer. **a)** The photovoltage signal measured as a function of Φ which is produced by the coupling of the fields shown in **b)**. [20]

As shown in Fig. 6, classical Michelson interfometry, which was developed from the Michelson-Morley experiment [28] uses a path length difference between waves to generate an interference pattern which can be used to determine the phase shift Ψ between two electric fields. In contrast spintronic Michelson interferometry as

shown in Fig. 7 controls the relative electromagnetic phase between the electric and magnetic fields in order to probe the material induced phase shift Φ between electric and magnetic fields at the permalloy ($Ni_{80}Fe_{20}$, Py) sensor. An Agilent E8257D microwave generator is used to provide a 0.2 - 20 GHz signal which is separated into two paths by an rf power splitter. One path travels through a phase shifter and is directly injected into the permalloy microstrip sensor, while the other path is shone on the sensor from a horn antennae. The magnetic field from the horn drives magnetization precession in the strip while the directly injected electric field produces a current. These two fields couple to produce a non zero dc voltage via the spin rectification effect which is detected by a Stanford Research SR830 DSP lock-in amplifier. By controlling the phase through the phase shifter inserted in one path, Φ can effectively be controlled and a signal analogous to the one shown in Fig. 7 a) can be measured. This allows the determination of Φ for the system. By sweeping the externally applied magnetic field (not shown in Fig. 7) an FMR spectra can also be obtained in the same system.

4.2 Lock-in Amplification

Since the voltages produced through the spin rectification effect based on AMR are quite small (a few μV) the dc signal will be obscured by background noise and a special technique is needed to extract the signal from the background. The technique which will be used is known as lock-in amplification. By modulating the input signal with a low frequency square wave set at some reference frequency, the dc output from the Py strip will also be modulated at the same frequency. However the noise will be unaffected. The lock-in amplifier then multiplies this signal by a sine wave of frequency equal to the reference frequency and averages over the signal using a low pass filter. Since sine waves of different frequencies are orthogonal, the noise will average to zero and only the signal at the reference frequency will remain. Thus the small dc signal can be measured with minimal background noise

5 Proposed Work

The goal of this work is to clearly demonstrate that the line shape of the electrically detected FMR depends on the phase Φ, ranging from purely symmetric when $\Phi = (2n+1)\frac{\pi}{2}$ to purely antisymmetric when $\Phi = n\pi$, $n = 0, 1, 2, ...$ and to demonstrate that the value of Φ does vary from one apparatus to another, showing the importance of phase characterization in FMR measurements. This will be done in three parts:

- Calculation of Φ in a simple thin film multilayer system for a plane wave incident normal to the surface of the thin layer
- Derivation of the FMR line shape beginning with the Landau Lifshitz equation for both in plane and out of plane field configurations showing the symmetric and antisymmetric dependence on Φ
- Fitting of experimental data to the determined line shape to demonstrate that Φ will change with experimental conditions

5.1 Φ in a Multilayer System

The first objective is to demonstrate that in a thin film multilayer system (such as those used in spin Hall effect experiments) there should in fact be a phase shift between the electric and magnetic fields. To do this we will consider the three systems shown in Fig. 8 a). The three structures will differ by the addition of a Pt layer and a tunneling MgO layer. In order to determine the phase shift Φ we will consider a plane wave incident from air perpendicular on the sample. The electric and magnetic waves in each layer must be calculated as the superposition of all reflected and transmitted waves from each of the other layers, which can be done by treating the wave in each layer as the sum of two waves, one moving in the positive direction and one in the negative direction. At each interface the boundary conditions of Maxwell's equations must be applied and using a transfer matrix method with the Fresnel coefficients

[27, 29], both the positive and negative moving waves can be determined. Using this method we will determine the relative phase in the permalloy layer. Since the phase

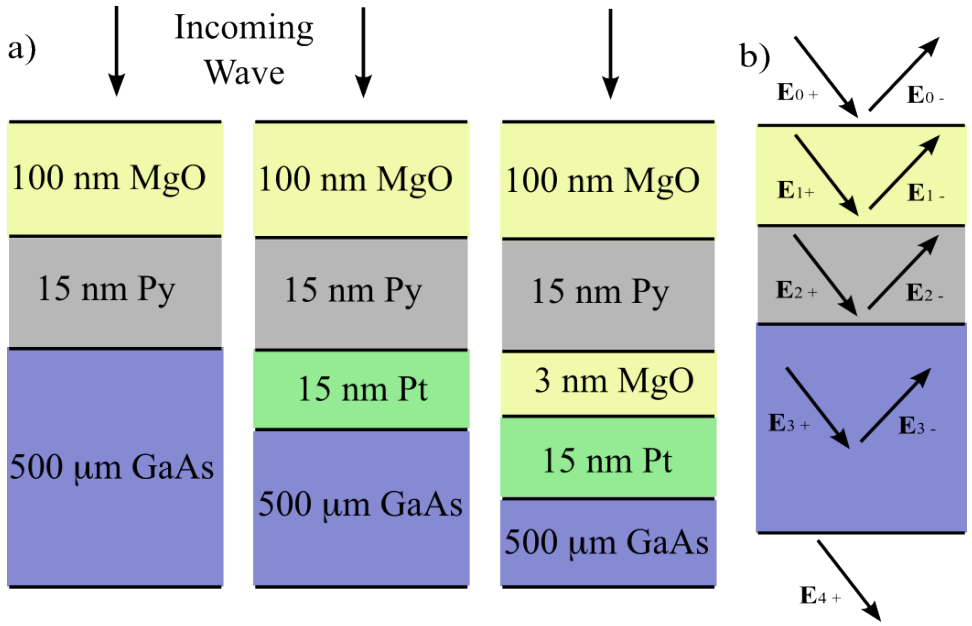

Figure 8: **a)** Three multilayer systems where Φ will be calculated in the Py layer. **b)** An illustration of the formalism of the matrix method using Fresnel coefficients.

shift will be induced by the imaginary part of the complex refractive index, we would expect that in the permalloy layer there is a phase shift between electric and magnetic fields, and that the addition of a platinum layer would increase the phase shift. The effect of adding a tunneling layer between the Py and Pt is somewhat less intuitive, and we will calculate Φ in this system for different thicknesses of the MgO layer to examine its effect.

The calculation of these waves in various layers is fairly straight forward if the material parameters of each layer are known, however it is a lengthy calculation involving numerous matrices and to compute Φ in the permalloy layer we will use Maple to do all calculations. This will also make the changing of material parameters, layer thicknesses and frequency of the field much easier. We will also perform simple

tests to see that the calculations make sense, such as setting all layers to have the same conductivity and using the well known formula for the phase shift in a uniform conductor of infinite extent to see that our calculations agree. From this step we will demonstrate that even in the simple case of a normally incident plane wave, the relative phase shift will be non zero and must be considered.

5.2 Line Shape for In Plane and Out of Plane Fields

Once we have demonstrated that Φ is in general nonzero, we then wish to show that the symmetry properties of the line shape depend on the relative electromagnetic phase. In order to do this we will begin with the Landau Lifshitz equation which will first be solved without damping to arrive at the Polder susceptibility tensor. This will relate the magnetization to the internal magnetic field, which will not be the same as the externally applied field. To relate the two we will use the boundary conditions of Maxwell's equations. We will then introduce damping phenomenologically to arrive at the Landau Lifshitz Gilbert equation and will show how the Polder tensor is modified with the addition of damping. The FMR line shape is determined from the generalized Ohm's law, and using our result for the damping modified Polder tensor we will find expressions for the photovoltage line shape for both the in plane and out of plane field configurations. Here it will be important to clearly demonstrate how the line shape can change with the phase Φ and to do so we will write the line shape in terms of its symmetric and antisymmetric Lorentz contributions. This means we will have to convert the Polder tensor from being expressed in terms of frequencies to being expressed in terms of magnetic fields and will explicitly use the real and imaginary parts of the susceptibility tensor elements rather than writing the expression in terms of the spin resonance phase, where the line shape dependence on Φ is hidden in the magnitude of the tensor elements. From this work we will see that since the relative phase is in general non zero, the AMR induced photovoltage will in general not be solely symmetric or antisymmetric.

5.3 Experimental Determination of Φ

Finally we want to show experimentally that Φ is indeed nonzero by fitting the measured line shape for different samples to the predicted line shape and determining the relative electromagnetic phase. To do this we will use the photovoltage line shape which we have derived to fit FMR spectra that have been collected over the past 4 years. This data was collected using the lock-in amplification technique described in section 4. Since we wish to illustrate the line shape dependence on Φ we will fit FMR data from different sample structures collected at different frequencies to see that Φ varies based on the sample preparation and experimental conditions. Specifically the data analyzed will be from spintronic sensors where the length of the Py strip varies from 200 μm - 2 mm, the width is 5 μm and the thickness is 100 nm. We will vary the frequency in 1 GHz steps from 2 to 10 GHz which will shift the resonant position and, as we will demonstrate, will also change the relative electromagnetic phase. For a fixed sample at fixed frequency we will also change the relative phase using spintronic Michelson interferometry and show that if the only parameter changed is Φ the line shape will still change. Such an analysis will be carried out for both in plane and out of plane configurations. In this way we will be able to show that we cannot assume that Φ is 0 in an arbitrary sample at an arbitrary frequency, but rather Φ must be determined experimentally.

5.4 Research Timeline

- December 27 - January 14
  - Determine the in plane and out of plane photovoltage expressions in terms of the symmetric and antisymmetric Lorentz line shape
  - Complete the theory portion of the thesis where these expressions are derived beginning with the Landau Lifshitz equation.
- January 14 - January 28:

  - Develop Maple script to calculate Φ in the permalloy layer of the three model systems based on the matrix method using Fresnel coefficients
  - Check calculation method in limiting case of infinite conductor to verify that the method is working
  - Examine the dependence of the relative phase on the addition of a Pt layer and a tunneling MgO layer of different thicknesses

- January 28 - February 18
  - Analyze data using Igor and determine Φ in various samples by fitting FMR line shape
  - Organize data to best emphasize how the symmetry properties of the FMR line shape depend on Φ
  - Begin work on paper for Physical Review B

- February 18 - February 28:
  - Prepare midterm presentation, begin work on final thesis and continue work on paper

- March:
  - Complete paper by early March
  - Work on written thesis and presentation, to be completed by the end of March

- April:
  - Submission of final thesis and defense

6 Significance

The goal of this research project is to demonstrate that the symmetry of the electrically detected ferromagnetic resonance line shape depends strongly on the relative electromagnetic phase Φ. This should radically change the way FMR experiments are viewed and performed since currently the effect of the relative phase is not considered seriously in most experiments. Even in spin Hall effect experiments where the AMR effect is acknowledged as contributing to the line shape, it has only been added as a convenient way of explaining the observed antisymmetric line shape and has not been included in its full generality. By demonstrating that in a multilayer system Φ is in general non zero, that the symmetry of the FMR line shape depends on this relative phase and that experimentally Φ varies between apparatus we will unambiguously demonstrate that to properly characterize the FMR line shape one must account for the relative electromagnetic phase. Thus our systematic demonstration of the effects of the relative phase will have an important impact on the condensed matter community. This work should be the first step in laying the foundation for a clear understanding of the electrically detected FMR line shape which will help resolve the controversy surrounding the experimentally measured values of the spin Hall angle. Once this first step has been established future work will involve determining how this understanding can be translated into an understanding of the spin Hall effect and how the AMR and spin Hall voltages can be experimentally distinguished in multilayer systems.

References

[1] N. Mo, C.E. Patton, *Local ferromagnetic resonance measurement techniques*, Rev. Sci. Instrum. **79**, 040901 (2008)

[2] Y.S. Gui, N. Mecking, X. Zhou, Gwyn Williams, C.-M. Hu, *Realization of a room-temperature spin dynamo: the spin rectification effect*, Phys. Rev. Lett. **98**, 107602 (2007)

[3] C. Kittel, *Introduction to Solid State Physics* (John Wiley & Sons, Inc., New York, 2004), 8^{th} ed.

[4] N. Mecking, A comprehensive study of the AMR-induced microwave photovoltage, photocurrent and photoresistance in Permalloy microwsrips, Ph.D. thesis, University of Hamburg

[5] B. Lax, K.J. Button, *Microwave Ferrites and Ferrimagnetics* (McGraw Hill, New York, 1962)

[6] R.W. Damon, *Ferromagnetic Resonance at high power* in *Magnetism, a treatise on modern theory and materials* (Academic Press, 1963)

[7] O. Mosendz, J.E. Pearson, F.Y. Fradin, G.E.W. Bauer, S.D. Bader, A. Hoffmann, *Quantifying Spin Hall Angles from Spin Pumping: Experiments and Theory*, Phys. Rev. Lett. **104**, 046601 (2010)

[8] J. Inoue, H. Ohno, *Taking the Hall Effect for a Spin*, Science **309**, 2004 (2005)

[9] Y. Tserkovnyak, A. Brataas, G.E.W. Bauer, *Spin pumping and magnetization dynamics in metallic multilayers*, Phys. Rev. B **66**, 224403 (2002)

[10] Y. Tserkovnyak, A. Brataas, G.E.W. Bauer, *Enhanced Gilbert Damping in Thin Ferromagnetic Films*, Phys. Rev. B **88**, 117601 (2002)

[11] X. Wang, G.E.W. Bauer, B.J. van Wees, A. Brataas, Y. Tserkovnyak, *Voltage Generation by Ferromagnetic Resonance at a Nonmagnet to Ferromagnet Contact*, Phys. Rev. Lett. **97**, 216602 (2006)

[12] A. Brataas, Y. Tserkovnyak, G.E.W. Bauer, B.I. Haperin, *Spin battery operated by ferromagnetic resonance*, Phys. Rev. B. **66**, 060404(R) (2002)

[13] L. Berger, *Generation of dc voltages by a magnetic multilayer undergoing ferromagnetic resonance*, Phys. Rev. B. **59**, 11465 (1999)

[14] T. Seki, Y. Hasegawa, S. Mitani, S. Takahashi, H. Imamura, S. Maekawa, J. Nitta, K. Takanashi, *Giant spin Hall effect in perpendicularly spin-polarized FePt/Au devices*, Nature Mater. **7**, 175 (2008)

[15] G. Mihajlovic, J.E. Pearson, M.A. Garcia, S.D. Bader, A. Hoffmann, *Negative Nonlocal Resistance in Mesoscopic Gold Hall Bars: Absence of the Giant Spin Hall Effect*, Phys. Rev. Lett. **103**, 166601 (2009)

[16] K. Ando, S. Takahashi, K. Harii, K. Sasage, J. Ieda, S. Maekawa, E. Saitoh, *Electric Manipulation of Spin Relaxation using the Spin Hall Effect*, Phys. Rev. Lett. **101**, 036601 (2008)

[17] T. Kimura, Y. Otani, T. Sato, S. Takahashi, S. Maekawa, *Room-Temperature Reversible Spin Hall Effect*, Phys. Rev. Lett. **98**, 156601 (2007)

[18] J.E. Hirsch, *Spin Hall Effect*, Phys. Rev. Lett. **83**, 1834 (1999)

[19] S. Zhang, *Spin Hall Effect in the Presence of Spin Diffusion*, Phys. Rev. Lett. **85**, 393 (2000)

[20] A. Wirthmann, Xiaolong Fan, Y.S. Gui, K. Martens, G. Williams, J. Dietrich, G.E. Bridges, C.-M. Hu, *Direct phase probing and mapping via spintronic Michelson Interferometry*, Phys. Rev. Lett. **105**, 017202 (2010)

[21] H.J. Juretschke, *Electromagnetic theory of dc effects in ferromagnetic resonance*, J. Appl. Phys. **31**, 1401 (1960)

[22] N. Mecking, Y.S. Gui, C.-M. Hu, *Microwave photovoltage and photoresistance effects in ferromagnetic microstrips*, Phys. Rev. B. **76**, 224430 (2007)

[23] M.I. D'yakonov, V.I. Perel, *Possibility of orienting electron spins with current*, Sov. Phys. JETP Lett. **13**, 467 (1971)

[24] M.I. D'yakonov, V.I. Perel, *Current-induced spin orientation of electrons in semiconductors*, Phys. Lett. A **35**, 459 (1971)

[25] Y. Kato, R.C. Myers, A.C. Gossard, D.D. Awshalom *Observation of the spin Hall effect in semiconductors*, Science **306**, 1910 (2004)

[26] J. Wunderlich, B. Kaestner, J. Sinova, T. Jungwirth, *Experimental observation of the spin Hall effect in a two-dimensional spin-orbit coupled semiconductor system*, Phys. Rev. Lett. **94**, 047204 (2005)

[27] O.S. Heavens, *Optical Properties of Thin Solid Films* (Dover, New York, 1965)

[28] A.A. Michelson, E.W. Morley *On the relative motion of the earth and the luminiferous ether*, Am. J. Sci. **34**, 333 (1887)

[29] M. Born, E. Wolf *Principles of optics: electromagnetic theory of propagation, interference and diffraction of light* (Oxford, New York, 1975)